β-Tetraethyl-β'-tetrapyridin-4-yl Porphyrins, Their N-Methylated Tetracations, and Heterodimers with *ms*-Tetraphenylsulfonato Porphyrins

Claus Endisch,[†] Jürgen-Hinrich Fuhrhop,*[,†] Jürgen Buschmann,[‡] Peter Luger,[‡] and Ulrich Siggel[§]

Contribution from the Institut für Organische Chemie and Institut für Kristallographie, der Freien Universität Berlin, Takustrasse 3, D-14195 Berlin, Germany, and Technische Universität Berlin, Max-Volmer-Institut für Physikalische Chemie, Strasse des 17, Juni 135, D-10623 Berlin, Germany

Received December 5, 1995[⊗]

Abstract: A mixture of the four regioisomers of β-tetraethyl-β'-tetrapyridin-4-yl porphyrins and their N-methylated tetracations has been synthesized. The crystal structure of regioisomer I is determined by complicated edge-on interactions between the pyridinyl substituents, which arrange as a "bowl". The nonseparable mixture of regioisomers III+IV is extremely well soluble in chloroform and, as tetramethylated tetracation, in water ($\cong 10^{-1}$ M). It forms well-defined and water-soluble (5×10^{-4} M) heterodimers with ms-tetraphenylsulfonatoporphyrin as a free base, a zinc and a copper complex ($K_{dimer} = 1.3 \times 10^{8}$ M^{-1}). Dimers containing one copper porphyrinate show no fluorescence. Cofacial porphyrin−porphyrin distances were estimated from transition dipole interaction as 7−8 Å. Tetracationic zinc porphyrinates are stable against acid demetalation, the corresponding free base is not protonated down to pH 1. NH-Deprotonation has been achieved with sodium hydroxide and leads to chain-like assemblies in water. Application of the new porphyrins in vesicle entrapment measurements, formation of electron donor−acceptor pairs, and molecular assemblies is shortly discussed.

Introduction

The large surface and planarity of the porphyrin chromophore favor strong van der Waals stacking interactions which lead to very large aggregates. Porphin and β-octamethylporphyrin are therefore insoluble in chloroform and other organic solvents.[1] The aggregations can, however, be halted at the stage of *homodimers*, if ethyl or larger alkyl substituents are introduced: porphyrin stacking between two molecules still occurs, but the side opposite to the porphyrin interaction is blocked.[1] Biologically active porphyrins therefore usually occur as dimers in solution,[1−4] protein matrices,[5] and crystals.[6,7] Prominent examples are the "special pair" of the chlorophylls[4,5] in solution and photosynthetic reaction centers and diamagnetic dimers of metalloporphyrin cation radicals in solution and in crystals.[8,9] Binding constants are usually in the order of 10^6-10^9 M.

We recently became interested in metalloporphyrin *heterodimers* in water showing similar binding constants of $\geq 10^6$ M for several reasons. We name three of them here: (i) For nucleic acid entrapment and release studies from lipsomes we need a simple spectroscopic method for measurements of entrapment volumes and membrane permeability of vesicle membranes. Such a test without gel chromatography is not known[10] but could easily be realized with a fluorescent, water-soluble porphyrin both in the bulk and vesicle entrapped water volumes, provided the porphyrin fluorescence in the bulk could be quantitatively quenched by addition of a copper porphyrinate counterion (Figure 1a). (ii) The intriguing possibility to produce phlorinradicals from tin(iv) porphyrinates and cation radicals from zinc porphyrinates[11] by irradiation of heterodimers with visible light cannot be studied with any of the existing heterodimers in water. Such a system is of interest, because the tin(iv) phlorinates are known to produce molecular hydrogen in the presence of colloidal platinum.[12] (iii) We needed a porphyrin counterion to cap fluorescent monolayer leaflets made of **1c** in water[13] with an electron trap.

Known heterodimers between tetracationic and −anionic porphyrins[14] or porphyrins and phthalocyanines[15] in water were tested but did not meet the requirements for such experiments. Fluorescence quenching in copper containing heterodimers was not quantitative and solubilities in water dropped to $\leq 10^{-5}$ M upon neutralization of charges. We therefore synthesized a mixture of four β-tetraethyl-β'-methylpyridinium porphyrins and studied its water-soluble heterodimers. It was found that the

* To whom correspondence should be addressed.
[†] Institut für Organische Chemie.
[‡] Institut für Kristallographie.
[§] Technische Universität Berlin.
[⊗] Abstract published in *Advance ACS Abstracts,* June 15, 1996.

(1) (a) Porphyrins and Metalloporphyrins; Smith, K. M., Ed.; Elsevier: Amsterdam, 1975. (b) Fuhrhop, J.-H. *Angew. Chem. Int. Ed. Engl.* **1976**, *15*, 648.
(2) Mauzerall, D. *Biochemistry* **1965**, *4*, 1801.
(3) (a) Gouterman, M.; Mathies, R. A.; Smith, B. E.; Caughey, W. S. *J. Chem. Phys.* **1970**, *52*, 3795. (b) Gouterman, M. *J. Chem. Phys.* **1959**, *30*, 1139.
(4) Katz, J. I.; Oettmeier, W.; Norris, J. R. *Philosoph. Trans. R. Soc. London* **1976**, Ser. *B 273*, 227.
(5) Deisenhofer, J.; Epp, O.; Miki, K.; Huber, R.; Michel, H. *Nature* **1985**, *318*, 618.
(6) Scheidt, W. R.; Lee, Y. J. *Struct. Bond.* **1987**, *64*, 24.
(7) Hunter, C. A.; Sanders, J. K. M. *J. Am. Chem. Soc.* **1990**, *112*, 5525.
(8) Fuhrhop, J.-H.; Wasser, P. K. W.; Riesner, D.; Mauzerall, D. *J. Am. Chem. Soc.* **1972**, *94*, 7996.
(9) Song, H.; Reed, C. A.; Scheidt, W. R. *J. Am. Chem. Soc.* **1989**, *111*, 6865.
(10) Lasic, D. D. Liposomes; *Elsevier*: Amsterdam, 1993.
(11) Fuhrhop, J.-H.; Kadish, K.; Davis, D. G. *J. Am. Chem. Soc.* **1973**, *95*, 5140.
(12) Krüger, W.; Fuhrhop, J.-H. *Angew. Chem., Int. Ed. Engl.* **1982**, *21*, 131.
(13) Endisch, C.; Böttcher, C.; Fuhrhop, J.-H. *J. Am. Chem. Soc.* **1995**, *117*, 8273.
(14) Ojadi, E.; Selzer, R.; Linschitz, H. *J. Am. Chem. Soc.* **1985**, *107*, 7783.
(15) Lipskier, J. F.; Tran-Thi, T. H. *Inorg. Chem.* **1993**, *32*, 722.

S0002-7863(95)04082-0 CCC: $12.00

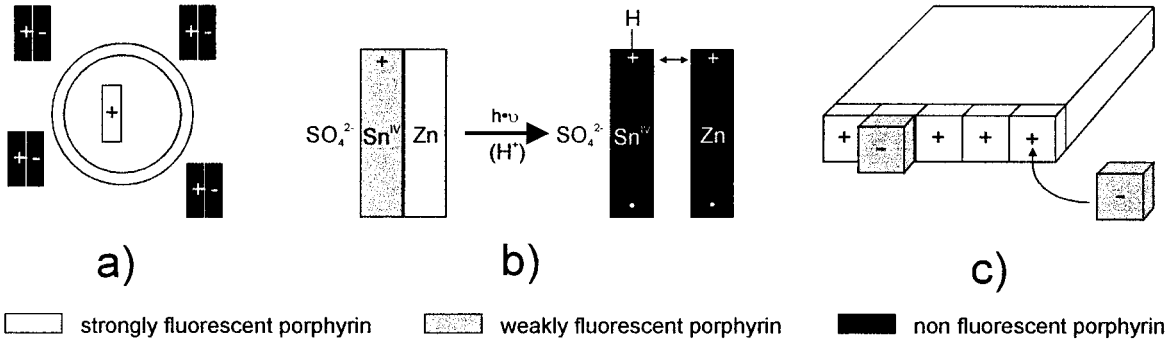

Figure 1. Some useful applications of metalloporphyrin heterodimers in bulk water (a) vesicle characterization by fluorescence quenching, (b) systematic studies of metalloporphyrin pairs in the ground and excited states, and (c) introduction of electron traps into photoactive porphyrin assemblies.

Table 1. Porphyrin Solubilities in Chloroform

porphyrin	solubility [mol·l^{-1}]
TETPyP I **1a**(I)	5.4×10^{-2}
TETPyP II **1a**(II)	1.5×10^{-3}
TETPyP III + IV **1a**(III+IV)	8.3×10^{-2}
TETPyP I−IV isomer mixture **1a**	8.5×10^{-2}
ms-TPyP **3**[23]	3.6×10^{-3}
OEP[1a]	1.1×10^{-2}

demands for the experiments sketched in Figure 1, namely binding constants $>10^6$ M, solubilites of $>10^{-4}$ M, and total fluorescence quenching are fulfilled by these dimers. Furthermore, both monomers are easily accessible, and aqueous standard solutions can be stored for long periods of time.

Results and Discussion

Synthesis, Isomer Separation, Solubilities, and a Crystal Structure. 4-(2-Nitro-but-1-enyl)pyridine and isocyanoacetic acid ethyl ester[16] were reacted in the presence of DBU in tetrahydrofuran to give 4-ethyl-3-pyridine-4-yl-1*H*-pyrrole-2-carboxylic acid ethyl ester in 81% yield.[17] Hydride reduction of the ethyl ester, cyclization to the porphyrinogens in acetic acid containing dimethoxymethane and *p*-toluenesulfonic acid and dehydrogenation with 2,3-dichloro-5,6-dicyanobenzoquinone (DDQ)[18] and chromatography yielded a total of 29% of porphyrin mixture **1**. Metalation and pyridine permethylation reactions to give **2** followed standard procedures (Chart 1). This compares favorably with syntheses of other water-soluble porphyrins. The mixture was separated into 9% of type I, 18% of types III+IV (nonseparable), 2% of type II in the order of elution. Water-soluble products were passed over a basic ion exchange column and precipitated with acetone. The metal complexes of the *meso*-substituted porphyrins **3**−**5** were prepared from the commercial porphyrins by standard procedures.[1]

The solubilities of isomers I, II, and III+IV of the β-tetraethyl-β-tetrapyridylporphyrin **1a** were determined by heating the porphyrins for 60 min in chloroform, filtering over Celite after 1 h and measuring the concentration by UV/vis spectroscopy (Table 1). *meso*-Pyridinylporphyrins **3** and β-pyridinylporphyrin **1**, isomer II, are of comparable solubility, namely $1-4 \times 10^{-3}$ M. β-Octaethylporphyrin is ten times more soluble and a factor of 30 is observed with the pure isomer I of **1** or an isomer mixture of III+IV or I+II+III+IV. In the case of isomer I, the unique crystal packing in orthogonal layers (see below) should be responsible for its outstanding solubility of 0.5×10^{-1} M. In the isomer mixtures, the unsymmetric distribution of substituents and the inseparable mixture of two regioisomers leads to a most useful inhibition of both homodimerization and crystal formation. This mixture is an ideal candidate for the formation of water-soluble heterodimers, because each individual isomer can interact in the same face-to-face geometry with *meso*-substituted porphyrins, e.g., **5**. The unwanted precipitation by charge-neutralization is much less likely than with a pure regioisomer.

Only the type I isomer of the β-tetraethyl-β'-pyridinylporphyrins (**1a**) could be crystallized. In the molecular structure all four pyridine rings have different tilt angles: 40.5, 54.2, 45.9, and 137.4° against the porphyrin plane, which is smaller than the usual 70° angle in *meso*-tetraphenylporphyrins.[6] Three rings are arranged propeller-like; the pyridine with the 137° angle interrupts this pattern. Regarding the pyridinyl substituents at diagonally opposite pyrrole rings, it is found that one pyridine pair is oriented in an orthogonal, the other in a parallel manner. The ethyl group neighboring the 137.4° pyridine unit is twisted down, whereas the other three ethyl groups are up. The crystal structure consists (i) of endless parallel columns of stacked molecules (not shown). In each column the porphyrin planes are all parallel, and the normal vector is at an angle of 45° to the column axis. All parallel, next neighbored molecules in a stack are symmetry-related to each other by an inversion center. Another consequence of the 45° angle between the stack axis and the normal of the molecular planes as well as of the short distance of 3.85 Å between the parallel planes of neighboring molecules is a side shift of 3.8 Å between them.[19] In order to characterize the relative positions of the pyridinyl substituents, we randomly selected one pyridine ring (= N40) as a central point of reference and depicted all neighboring pyridine units with a center to center distance of less than 6.7 Å. We found eight such neighbors (A−H, Figure 2). Two pyridine rings A and B lie perpendicular to each other as observed in *meso*-tetraphenylporphyrin,[20] but they are oriented edge-on and lie on both sides of the N40 pyridine plane. They belong to the same porphyrin stack as the N40 ring. Neighboring porphyrin stacks then provide four more pyridine rings, E, F, G, and H, which lie at an inclination angle of about 60°. This arrangement corresponds to the one found in the crystal structure of pyridine.[21] The orthogonal ring pair C and D finally complete a "bowl" around the reference pyridine ring.

(16) (a) Hartman, G. D.; Weinstock, L. M. *Organic Syntheses Coll*. **1988**, *6*, 620. (b) Obrecht, R.; Herrman, R.; Ugi, I. *Synthesis* **1985**, 400.

(17) (a) Barton, D. H. R.; Zard, S. Z. *J. Chem. Soc. Chem. Commun.* **1985**, 1098. (b) Barton, D. H. R.; Kervagoret, J. S. Z. Zard, *TH* **1990**, *46*, 7587. (c) Ono, N.; Maruyama, K. *Bull. Chem. Soc. Jpn.* **1988**, *61*, 4470. (d) Ono, N.; Kawamura, H.; Maruyama, K. *Bull. Chem. Soc. Jpn.* **1989**, *6*, 3386.

(18) (a) Ono, N.; Kawamura, H.; Bougauchi, M.; Maruyama, K. *J. Chem. Soc., Chem. Commun.* **1989**, 1580. (b) Ono, N.; Kawamura, H.; Boughauchi, M.; Maruyama, K. *TH* **1990**, *46*, 7483.

(19) A more detailed discussion and experimental data on the molecular and crystal structures are provided as additional material.

(20) Byrn, M. P.; Curtis, C. J.; Sawin, P. A.; Tsurumi, R.; Strouse, C. E. *J. Am. Chem. Soc.* **1990**, *112*, 1865.

(21) Mootz, D.; Wussow, H.-G. *J. Chem. Phys.* **1981**, *75*, 1517.

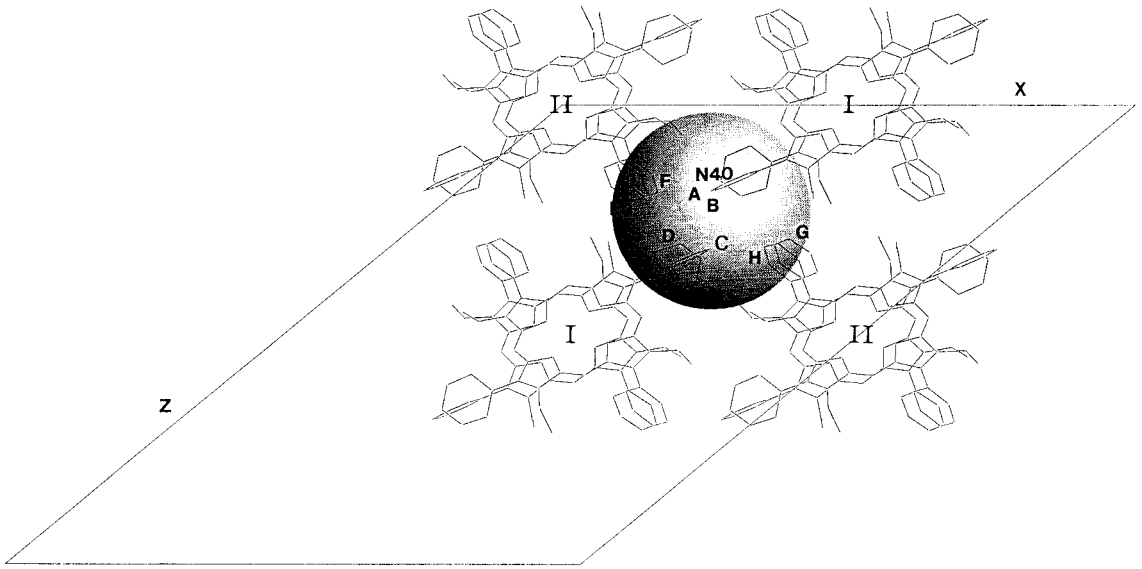

Figure 2. Unit cell projection of free base *β*-tetraethyl-*β′*-tetrapyridinylporphyrin **1a**,I down the *y*-axis. Viewing direction is parallel to the stacks I and II, which lie perpendicular to each other in different planes. A−H indicate eight pyridine rings lying close to the pyridine ring N40 (distance ≤ 6.7 Å). They form a bowl around it symbolized by the grey sphere.

Chart 1

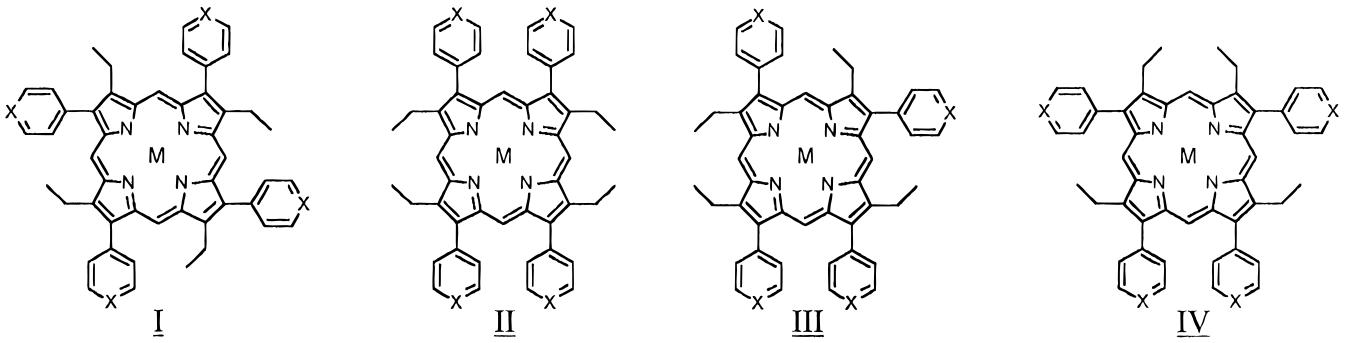

1 : X = N

2 : X = $\overset{\oplus}{N}$-CH_3

a : M = 2H; b : M = Cu(II); c : M = Zn(II); d : M = Sn(IV)Cl_2

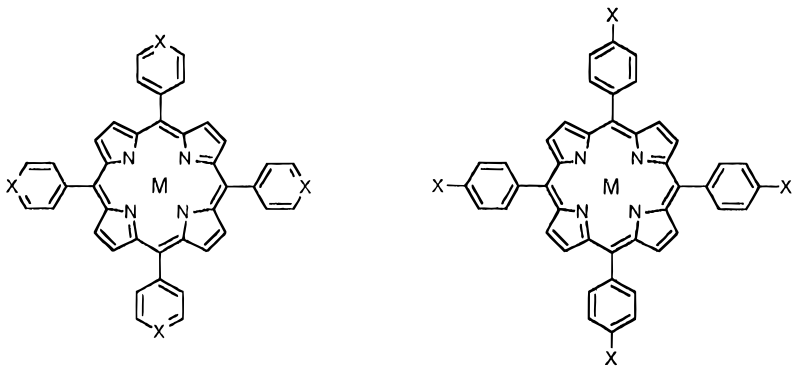

3 : X = N

4 : X = $\overset{\oplus}{N}$-CH_3

5 : X = SO_3^-

a : M = 2H; b : M = Cu(II); c : M = Zn(II); d : M = Sn(IV)Cl_2

Spectra, pk_as and Zinc Complex Stability. N-Methylation of the pyridine substituents renders the *β*-pyridinyl porphyrins **1a**−**d** water-soluble and produces electron accepting pyridinium rings. Distinct differences appear between the Soret bands of

Table 2. Quantitative UV−vis Spectra of β-Tetraethyl-β'-tetrapyridinyl Porphyrins **1** and Their Tetramethylated Pyridinium Derivatives **2**

compound, isomer, metal ion	N-band		Soret (B)-band	$\Delta\lambda_{1/2}$	Qy-band		Qx-band		solvent
TETPyP I **1a**(I)			412	26	506	540	576	628	$CHCl_3$
			2.33×10^5		1.78×10^4	1.13×10^4	7.70×10^3	3.85×10^3	
TETPyP II **1a**(II)			413	27	506	540	576	628	$CHCl_3$
			2.12×10^5		1.73×10^4	1.08×10^4	7.58×10^3	3.79×10^3	
TETPyP III + IV			412	26	506	540	575	628	$CHCl_3$
1a(III+IV)			2.38×10^5		1.85×10^4	1.19×10^4	8.21×10^3	4.51×10^3	
TETPyP III + IV Cu	330	386 (sh)	409	13	532		569		$CHCl_3$
1b(III+IV)	1.90×10^4	4.00×10^4	3.43×10^5		1.57×10^4		2.59×10^4		
TETPyP III + IV Cu	333	386 (sh)	411	19	535		570		DMSO
1b(III+IV)	2.41×10^4	3.22×10^4	2.47×10^5		1.49×10^4		1.98×10^4		
TETPyP III + IV Zn	335	391 (sh)	413, 425(sh)	19	541, 554(sh)		575, 591(sh)		$CHCl_3$
1c(III+IV)	2.16×10^6	3.39×10^4	2.23×10^5		1.32×10^4		1.44×10^4		
TETPyP III + IV Zn	337	401 (sh)	425	13	549		584		DMSO
1c(III+IV)	2.92×10^4	4.94×10^4	3.43×10^5		2.13×10^4		1.51×10^4		
TETPyP III + IV $SnCl_2$	364	399	420	11	546		584		DMSO
1d(III+IV)	2.20×10^4	4.34×10^4	3.21×10^5		1.83×10^4		9.92×10^3		
TETPyP III + IV	342		426	32	515	551	583	637	MeOH/H_2O 1:1
1a(III+IV)									pH = 1,0
2(III+IV)		387(sh)	437	34	570		612		DMSO, $KOBu^t$
dianion									
2a(III+IV)	340		425	34	517	554	576	629	H_2O
	3.65×10^4		1.45×10^5		1.30×10^4	9.56×10^3	8.25×10^3	2.99×10^3	
2a(III+IV)	350		429	37	518	553	581	639	MeOH/H_2O 1:1
	4.42×10^4		1.53×10^5		1.65×10^4	1.23×10^4	9.77×10^3	4.63×10^3	
2a(III+IV)	344		431	32	517	553	584	638	DMSO
	3.77×10^4		1.70×10^5		1.62×10^4	9.80×10^3	7.84×10^3	2.34×10^3	
2b(III+IV)	340		430	38	548		587		H_2O
	3.84×10^4		1.22×10^5		1.43×10^4		1.73×10^4		
2b(III+IV)	330		430	38	547		587		MeOH/H_2O 1:1
	4.03×10^4		1.34×10^5		1.52×10^4		2.06×10^4		
2b(III+IV)	337		438	36	549		588		DMSO
	4.59×10^4		1.58×10^5		2.20×10^4		2.34×10^4		
2c(III+IV)	338		442	38	560		600		H_2O
	4.46×10^4		1.31×10^5		1.77×10^4		1.35×10^4		
2c(III+IV)	338		448	38	564		604		MeOH/H_2O 1:1
	4.93×10^4		1.36×10^5		1.93×10^4		1.58×10^4		
2c(III+IV)	340		450	31	563		603		DMSO
	4.90×10^4		1.75×10^5		2.16×10^4		1.54×10^4		
2d(III+IV)	346	410(sh)	433	16	555		594		DMSO
	1.61×10^4	2.50×10^4	1.73×10^5		1.19×10^4		5.01×10^3		

β-pyridinylporphyrins **1** and their tetramethylated pyridinium derivatives **2** (TETMePyP) in DMSO. The electroneutral porphyrins and their metal complexes always show a narrow band ($\Delta\lambda^1/_2 = 13-26$ nm) in the region between 412 and 425 nm, whereas the tetracationic pyridinium compounds exhibit extensive line broadening ($\Delta\lambda^1/_2 = 32-36$ nm) accompanied by a corresponding decrease in intensity as well as a red shift of 13−27 nm. In the electron-rich zinc porphyrinate, for example, a 25 nm bathochromic shift is accompanied by broadening by a factor of 2.3. This effect cannot be caused by aggregation and excitonic interactions, since the fluorescence spectra show no dilution effect in the concentration range of $10^{-8}-10^{-4}$ M. In the *meso*-substituted pyridinium porphyrins, a small red shift of 2 nm has been attributed to dimerization, which may also be the order of magnitude for such an effect in our compounds.[22]

The pk_a of the pyrrole protonations in the porphyrin center drops from 5 in β-octaethylporphyrin to 0.5 for the monocation and −0.2 for the dication in β-tetramethylpyridinium as well as in the nonmethylated β-tetrapyridinium porphyrins. The pyridine nitrogen atoms are thus protonated before the central pyrrole nitrogens. Only in ≥5 M hydrochloric acid, did the two-banded spectrum of the diprotonated porphyrin dication appear, which corresponds to observations in *meso*-tetrapyridinium porphyrins.[23] The zinc complex of the tetracationic β-tetramethylpyridinium isomer **2c**, III−IV mixture was also dissolved in dilute hydrochloric acid. Down to pH 1.0 there was no sign of demetallation detectable by visible spectroscopy after one day. The zinc complex of the *ms*-tetraphenylsulfonato porphyrin **5c** was demetalated within a few minutes already at pH 2, whereas the more closely related *ms*-tetramethylpyridinium porphyrin **4c** lost about 5% of its central zinc ion within a day at pH 1. This complex has already been used in attempts to realize oxygen evolving systems at pH 1.6.[24]

The properties of the β-tetramethylpyridinium porphyrins in the ground and excited states clearly demonstrate that much of the π-electron density of the porphyrin is distributed into the methylpyridinium substituents. The long wavelength shift is then caused by a partial conjugation of the porphyrin and pyridinium π-systems, the line broadening by resulting sterical repulsion effects and porphyrin puckering, the lowering of the pk_a by massive loss of electron density of the central nitrogen atoms. These effects are less pronounced in the *meso*-substituted analogues.

The conjugation effect also lowers the thermodynamic stability of the metal complexes. We prepared these chelates with the best results, when we introduced the metal ions into

(22) Brookfield, R. L.; Ellul, H.; Harriman, A. *J. Photochem.* **1985**, *31*, 97.

(23) Fleischer, E. B. *Inorg. Chem.* **1962**, *1*, 493.

(24) Borgarello, E.; Kalyanasundaram, K.; Okuno, Y.; Grätzel, M. *Helv. Chim. Acta* **1981**, *64*, 1937.

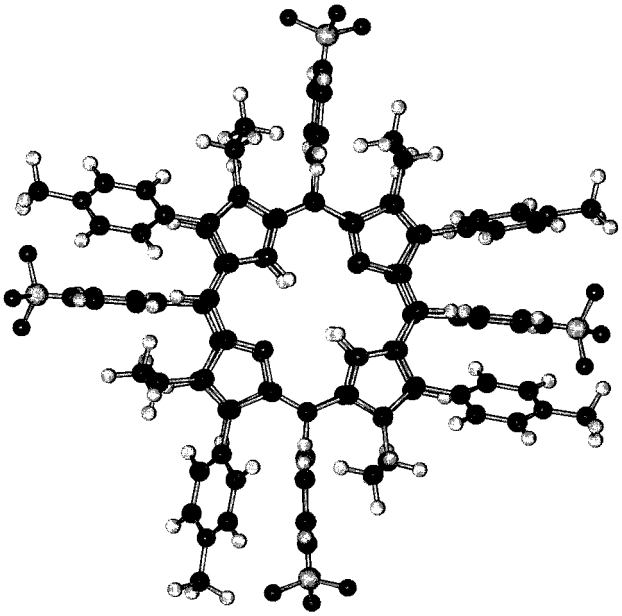

Figure 3. Hypothetical structure of heterodimer **1a**, III with **5a**. The chromophore distance is about 7 Å.

the electroneutral *β*-pyridinyl porphyrins, and methylated them afterwards. Nevertheless the zinc complexes are extraordinarily long-lived in strongly acidic solutions, because the four nitrogen atoms have very little affinity to protons (see also Figure 9). Acid stability of the metal complexes is thus probably of kinetic origin. It is a most useful property in respect to the construction of metalloporphyrin monolayer leaflets made of **1a**,**II**, which are most stable at pH 2.5[13] (see also Figure 1).

Heterodimers. We investigated the *β*-ethyl-*β*′-methylpyridinium porphyrins **2a**−**c** in the heterodimerization with *ms*-tetraphenylsulfonatoporphyrins **5a**−**c**. We used the free bases (B1 and B2, the zinc (Zn1 and Zn2), and the copper(II) (Cu1 and Cu2) complexes of both porphyrins and titrated all nine possible pairs: B1 B2; B1 Zn2; B1 Cu2; Zn1 Zn2; Zn1 Zn2; Zn1 Cu2; Cu1 Cu2; B2 Zn1, and B2 Cu1. Methanol−water (1:1)[22,26−28] was chosen as solvent, because homodimers of **2** are less stable in this solvent mixture than in pure water. The interpretation of spectroscopic changes, in particular, titration points corresponding to a large excess of **2a**−**c**, and the application of the exciton theory were less complicated than with the data obtained in water. All heterodimers can, however, also be cleanly produced in pure water or in DMSO at a 1:1 ratio of monomers. Figure 3 shows the most likely structure of a heterodimer of isomer III of **2a** with TPPS **5a**.

The most pronounced effects on the Soret absorption and fluorescence bands upon mixing were observed with the zinc *β*-methylpyridinium and copper *ms*-phenylsulfonatoporphyrins (**2c** + **5b**). Both the Soret bands and the Q-bands of both partners lost intensity upon mixing (Figure 4a). Addition of sodium perchlorate gave back the original spectra of the separated compounds (Figure 4a), because it leads to counterion stabilized homodimers of **2c**. Since the dimerization effects are so pronounced in the pair **2c** + **5b** we chose it as a model for the interpretation of the spectra and for the establishment of heterodimer formation. Spectroscopic titration gave sharp

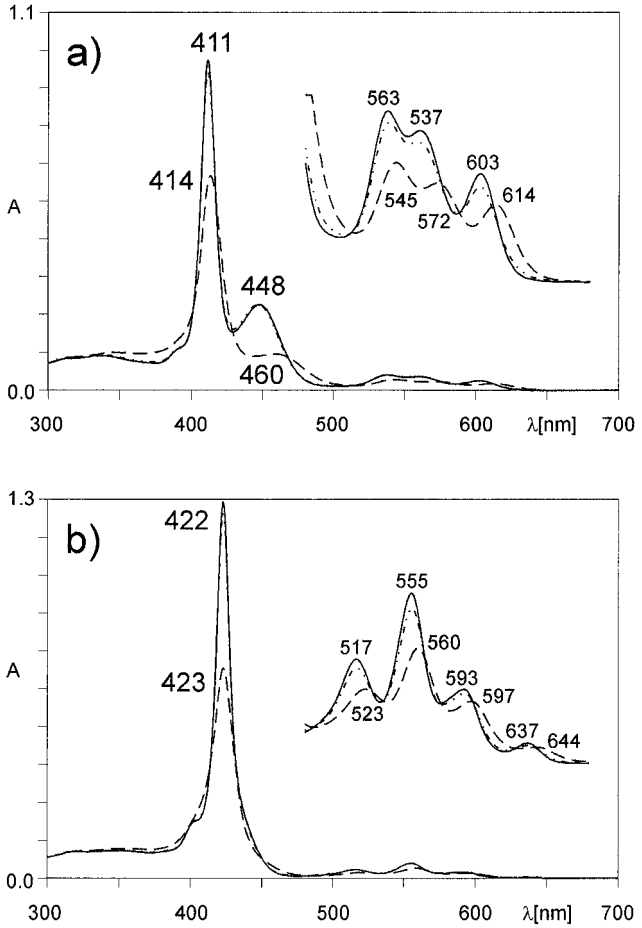

Figure 4. Two-component UV/vis spectra: (—) separated, (– ——) mixed; (– · –) mixed plus sodium perchlorate (0.1 M); solvent: methanol:water 1:1. (a) Zinc *β*-pyridinium porphyrinate **2c**, isomers III+IV and copper *ms*-tetraphenylsulfonatoporphyrinate **5b** and (b) corresponding free base **2a** + zinc complex **5c**.

isosbestic points, suggesting the formation of only the desired heterodimer (Figure 5). The pair made of the zinc-*ms*-sulfonate **5c** and free base *β*-pyridinium **2a**, on the other hand, gave no red-shifted Soret band because its transition moment approaches zero (Figure 4b). Only diminution of the Soret band intensity of Zn TPPS was observed and again reversed by sodium perchlorate.

The assumption of a heterodimer was first verified by the usual method of continuous variations (Job plot) and the expected minimum at a 1:1 ratio of two free porphyrin bases (Figure 6a) or a metalloporphyrin pair (Figure 6b). The slopes are not always constant (Figure 6a) since some dissociation takes place. In the zinc−copper porphyrin pair one finds two slopes on the left branch of the Job plot (Figure 6b). At high concentrations of **2c** $CuTPPS^{4-}$ (**5b**) can take up two of the *β*-zinc porphyrins, one on each surface of the *meso*-substituted porphyrin. A 2:1 complex is formed to some extent. Upon addition of equimolar amounts of **5b**, however, the trimer splits to form a 1:1 heterodimer. On the right branch of the same plot, where the *ms*-tetraanion is always in excess, no such break in the slopes is observed (Figure 6b). The isosbestic points are observed in both titrations (Figure 3), which means that the spectra of the trimer (**2c**/**5b**/**2c**) and the dimer (**2c**/**5b**) are very similar. The occurrence of the trimer as an intermediate is also confirmed by fluorescence titrations (see below).

The spectroscopic effects caused by heterodimerization have been interpreted here with a specially fitted exciton theory. van

(25) Shimidzu, T.; Iyoda, T. *Chem. Lett.* **1981**, 853.
(26) Vergeldt, F. J.; Koehorst, R. B. M.; Schaafsma, T. J.; Lambry, J. C.; Martin, J.-L.; Johnson, D. G.; Wasielewski, M. R. *Chem. Phys. Lett.* **1991**, *182*, 107.
(27) Geiger, D. K.; Kelly, C. A. *Inorg. Chim. Acta* **1988**, *154*, 137.
(28) Hofstra, U.; Koehorst, R. B. M.; Schaafsma, T. J. *Magn. Res. Chem.* **1987**, *25*, 1069.

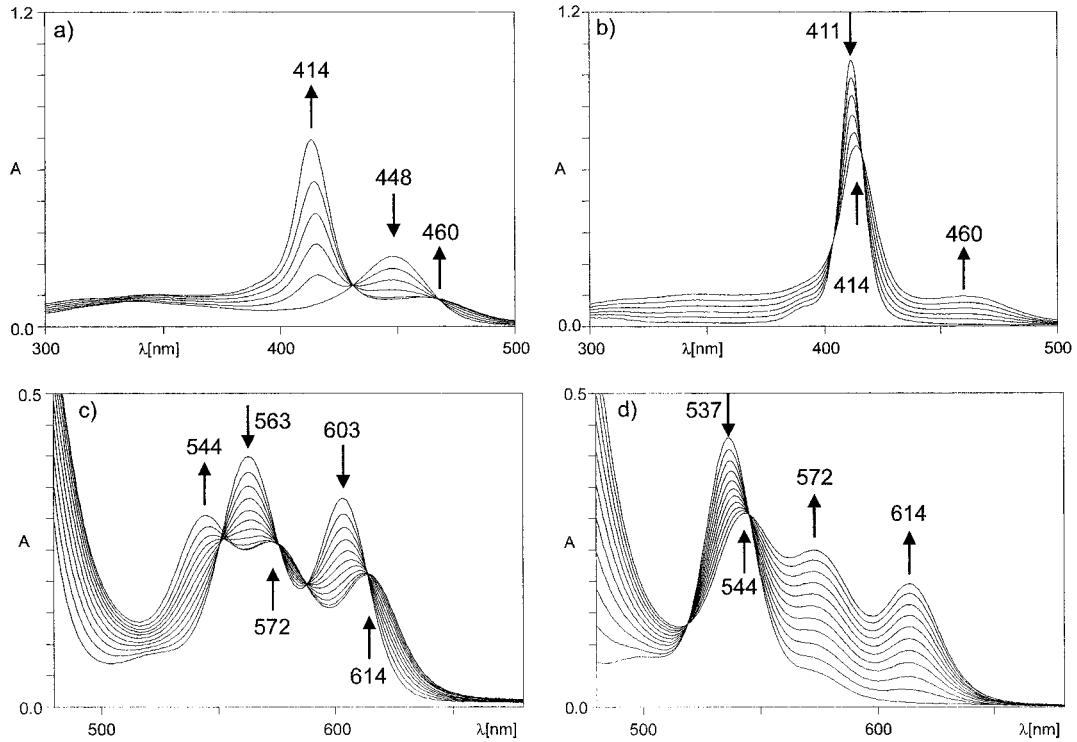

Figure 5. Spectrophotometric titrations corresponding to Figure 4a. (a,c) Titrations of zinc tetrapyridinium porphyrin **2c** with copper tetraphenylsulfonatoporphyrin **5b**; 2×10^{-6} and 2×10^{-5} M. (b,d) Titrations of **5b** with **2c**; 2×10^{-6} and 2×10^{-5} M.

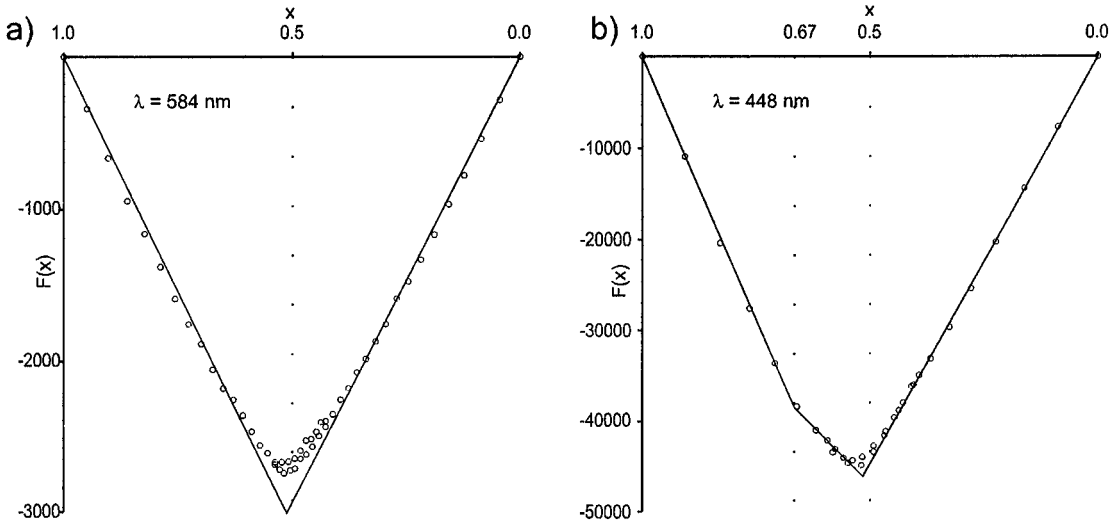

Figure 6. Job plots corresponding to (a) free bases **2a** + **5a** and (b) two metal complexes **2c** + **5b** (see Figure 5).

Table 3. Calculated Exciton Splittings and van der Waals Shifts for All Heterodimers (**2a**−**c**) + (**4a**−**c**)

	β-Zn/ms-Cu	β-Zn/ms-H_2	β-Zn/ms-Zn	β-Cu/ms-Cu	β-H_2/ms-Cu	β-H_2/ms-H_2	β-H_2/ms-H_2	β-H_2/ms-Zn	β-Cu/ms-Zn
E_1[a]	24331	24155	23697	24331	24331	24155	24155	23697	23697
E_2[a]	22321	22321	22321	23256	23310	23256	23310	23310	23256
ΔE	2009	1833	1375	1075	1021	899	845	387	441
E_b	24155	24030	23529	24727	24272	24155	24155	23641	
E_r	21739	21810	21930	21978	22222	22523	22222	22222	
V_{12}	670	633	408	1013	889	681	869	682	
V_s	−379	−314	−279	−668	−573	−367	−544	−572	

der Waals interactions are also considered. The symmetric splitting of the excited state energy levels into a lower and upper level in homodimers changes in heterodimers to an asymmetric splitting and is determined by both the exciton energy V_{12} and the difference in excitation energies of the monomers ΔE (Table 3, Figure 7). The excitation energy is now localized on one molecule with little admixture of the other molecule to the common excited state. In homodimers the upper energy level is allowed, the absorption band is blue-shifted, and the red-shifted band is symmetry forbidden. In heterodimers, on the other hand, the red-shifted band becomes partly allowed and gains in intensity. In our case it appears as a separate peak or as a shoulder of low intensity at about 450−460 nm.

In order to fit the observed UV/vis spectra, strong van der Waals interaction causing a red shift must also be assumed (formula in Figure 7).

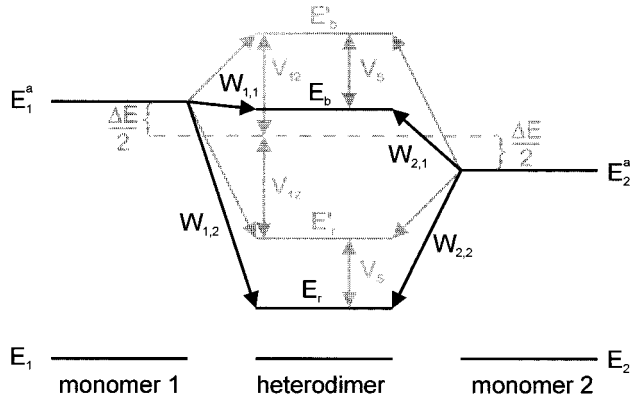

$$W_{1,1} = -\frac{\Delta E}{2} + \sqrt{\frac{\Delta E^2}{4} + V_{12}^2} + V_S \qquad \Delta E = (E_1^a - E_1) - (E_2^a - E_2)$$

$$W_{1,2} = -\frac{\Delta E}{2} - \sqrt{\frac{\Delta E^2}{4} + V_{12}^2} + V_S \qquad V_s = \frac{W_{1,1} + W_{1,2} + \Delta E}{2}$$

$$V_{12} = \frac{1}{2}\sqrt{(W_{1,1} - W_{1,2})^2 - \Delta E^2}$$

Figure 7. Energy diagram of a heterodimer including the ground state E_1, E_2, and the excited state levels of monomer 1 and 2. The grey lines show the asymmetric splitting of the excited state levels as determined by the exciton interaction energy V_{12}. The asymmetry is produced by the difference ΔE of transition energies of the monomers. The black lines include the additional van der Waals shift V_s leading to E_b and E_r which correspond to the experimental values of the excited states. The W values represent the modification of the transition energies of the monomers upon heterodimerization.

An especially clearcut example for the analysis of the Soret band splitting in porphyrin heterodimers is again given by the zinc pyridinium **2c** and copper *ms*-sulfonate **5b** pair. The difference between the exitation energies ΔE of the monomers has the largest value of all the pairs (2009 cm^{-1}). Accordingly, the red-shifted Soret band at 460 nm is most intense here. The pair **5c**/**2a**, on the other hand, produces a minimum value for ΔE (387 cm^{-1}) and only a small shoulder at 450 nm.

The results of the evaluation are summarized in Table 3. The highest exciton interaction energy V_{12} is calculated for the Cu−Cu dimer (1010 cm^{-1}), the lowest for the **2c** + **5c** pair (410 cm^{-1}). The calculated van der Waals shifts vary between −280 and −670 cm^{-1} parallel to the van der Waals interaction. It also becomes evident that in all heterodimers containing the zinc β-pyridinium porphyrinate **2c** excitation splitting is small. The metalloporphyrin with the strongest intramolecular π−π interactions between the porphyrin chromophore and its pyridinium substituents (Soret band at 448 nm) is obviously less efficient in exciton coupling than the free base or the copper complex, where much smaller Soret band shifts are observed.

Since the transition moments as deduced from the Soret bands are essentially the same for all the porphyrins used, the differences in excitation interaction should reflect either a lateral shift in the face-to-face arrangement or differences in the distances. The symmetrical arrangement of the four charges hardly allows lateral shifts. The distance in a face-to-face dimer can be calculated from the interaction energy using a simple point dipole formula and the formula of Gouterman[3] for the transition dipole moments. The result is 6.7 Å for the copper dimer (**2b**/**5b**) and 7.9 Å for the β-Zn/ms-free base pair (**2c**/**5a**). The (squared) transition moments applied were 54.4 (Cu-β **2b**), 67.4 (Cu-*ms* **5b**), 53 (Zn-β **2c**), and 71.1 D^2 (H_2-ms **5a**).

A second method to study dimerization and subsequent larger assemblies consists in the measurement of fluorescence intensities. The evaluation is especially easy if one of the parent compounds is a copper porphyrin. In the monomers the unpaired electron of copper couples to both the singlet and triplet

$$V_{12} = \frac{M_1 \cdot M_2}{r^3}$$

$$M^2 = \frac{1}{2} \cdot \frac{e^2 \cdot \epsilon \cdot \Delta\lambda_{1/2}}{\lambda_{max} \cdot 2510}$$

excited states of porphyrins.[3] Fluorescence is quenched completely. Our heterodimers fluoresce, but fluorescence is totally quenched if one of the components is a copper porphyrin. This is different from heterodimers containing two *meso*-substituted porphyrins or a copper(II) phthalocyanine where smaller quenching efficiencies are observed.[15] The mechanism of the intermolecular fluorescence quenching is not known, but our case, namely face-to-face stacking of two porphyrins without rotational displacement, is obviously optimal for the interaction of both π-orbitals with the unpaired dz^2-electron of the one central copper(II) ion.

We consider the quantitative quenching of porphyrin fluorescence in highly diluted aqueous solutions as an important tool in molecular assembly chemistry and therefore studied it in detail. We have detected two types of titration curves. One was realized upon titration of β-pyridinium porphyrins **2a** or **2c** with the copper-*ms*-sulfonato porphyrin **5b**. In this case the copper porphyrin quenched very effectively at a 1:1 ratio of porphyrins: The fluorescence of **2c** was only 0.8% at 10^{-5} M and 4.5% at 10^{-6} M. A plot of the relative fluorescence intensity in dependence of the copper porphyrin/porphyrin ratio shows an initial slope of 1.69 (Figure 8a). A slope of 1 would correspond to an aggregate of 1:1 stoichiometry and negligible dissociation, a slope of 2.0 would indicate a trimer with a central copper porphyrinate. The actual slope of 1.69 therefore shows that although at the beginning of the titration there is a large excess of **2c** over the copper porphyrin the equilibrium constant is not large enough for the quantitative formation of the trimer. In the course of titration binding charge interactions to both cationic surfaces of the trimer become stronger and the trimers successively lose one of the β-pyridinium porphyrins. The titration curve can be described by the formula below which is based on the assumption that the fluorescence intensity is proportional to the concentration of porphyrin **2**. As formation constants K_1 and K_2 for the dimer and trimer we determined $K_1 = 1.3 \times 10^8$ M^{-1} and $K_2 = 1.4 \times 10^5$ M^{-1}.

$$\frac{c_2^\circ}{c_1^\circ} = \left(\frac{F_{max}}{F} - 1\right) \cdot \frac{\left(\frac{F}{F_{max}}\right)^2 + \frac{1}{K_2 c_1^\circ}\left(\frac{F}{F_{max}} + \frac{1}{K_1 c_1^\circ}\right)}{2 \cdot \frac{F}{F_{max}} + \frac{1}{K_2 c_1^\circ}}$$

The second type of titration curve was encountered when *ms*-sulfonato porphyrins **5a** or **5c** were titrated with the copper β-pyridinium porphyrin **2b**. In this type of pairing, copper porphyrin quenched much less effectively than in the first case. At a 1:1 ratio of the porphyrins the fluorescence of **5a** is 11% and 21.8% at 10^{-5} and 10^{-6} M, respectively. Complete quenching was only achieved with an excess of 20 and 40% of the copper porphyrin **3b**. As long as the concentration of the copper complex **2b** is kept low, only the dimer is formed (Figure 8b). Because of some problems to fit the whole titration curve, only a lower limit for the formation constant $K_1 \geq 5 \times 10^6$ M^{-1} could be determined.

The results of the fluorescence titrations also show unequivocally that the 1:1 molecular assembly of **2c** + **5b** corresponds to dimers only, not to oligomers.

Base Titrations. In DMSO solution containing potassium *tert*-butoxide the β-tetramethylpyridinium porphyrin **2a** produces

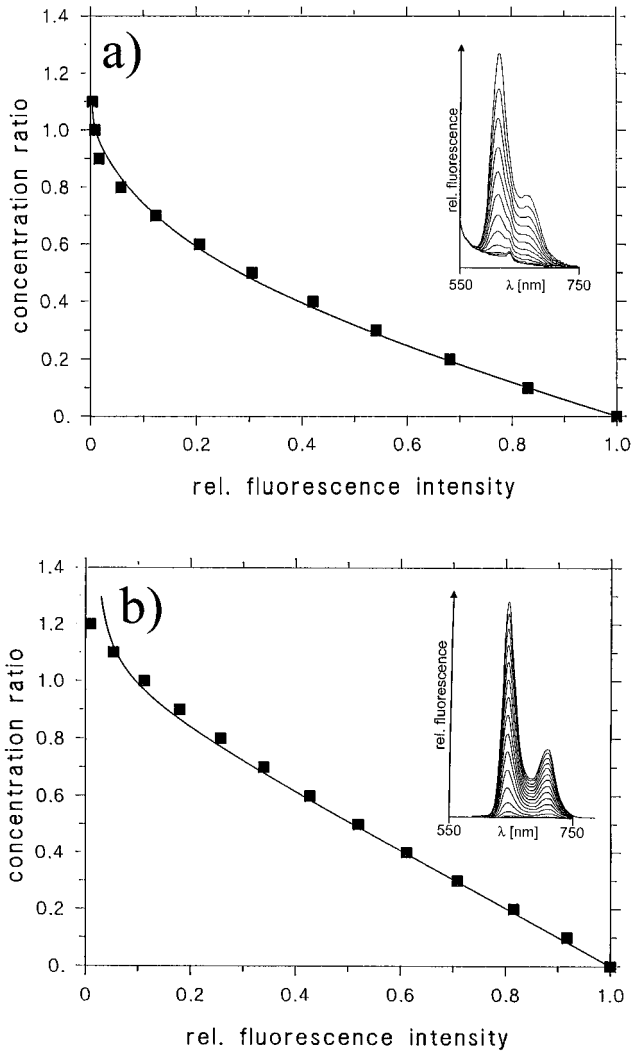

Figure 8. Relative fluorescence intensities in the titration of two heterodimer pairs containing one copper porphyrinate. (a) Zinc tetrapyridinium porphyrin **2c** 2×10^{-5} M with copper tetraphenylsulfonatoporphyrin **5b** 1×10^{-4} M, $\lambda_{Ex} = 530$ nm (b) free base *meso*-tetraphenylsulfonatoporphyrin **5a** 2×10^{-5} M with copper tetrapyridinium porphyrin **2b** 1×10^{-4} M, $\lambda_{Ex} = 414$ nm.

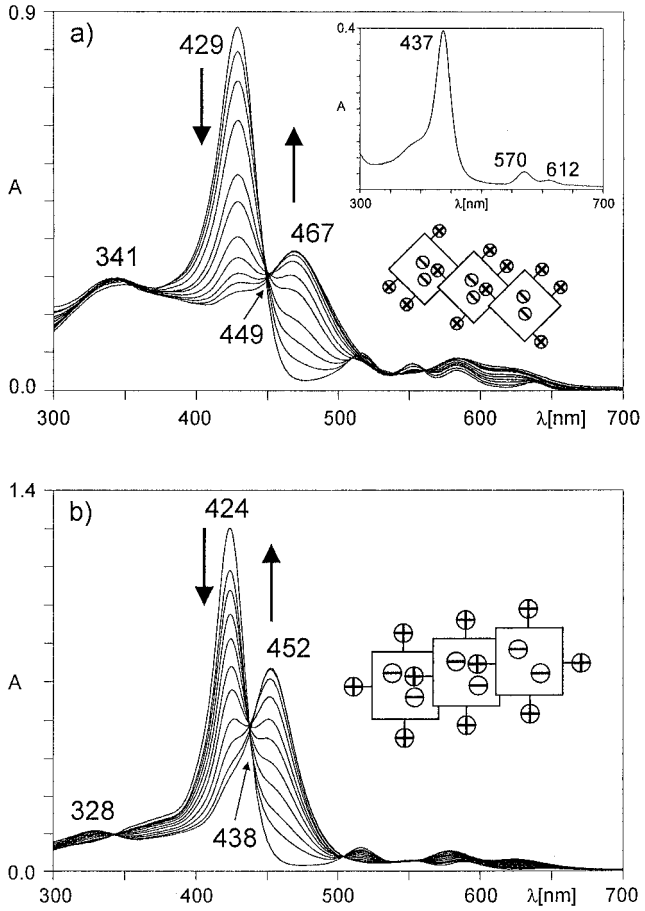

Figure 9. UV/vis spectra of (a) β-tetraethyltetramethylpyridinium porphyrin isomer mixture III+IV and (b) *meso*-tetramethylpyridiniumporphyrin **4a** in methanol/water 1:1 upon titration with sodium hydroxide. The models shown indicate the assumed structure of the lateral porphyrin assemblies. The inserted spectrum in (a) gives the monomeric porphyrin dianion spectrum in DMSO/potassium *tert*-butoxide.

the deprotonated dianion with two visible absorption bands at 512 and 570 nm and a Soret band at 437 nm ($\Delta\lambda^1/_2 = 34$ nm; see inset in Figure 9a). In methanol/water = 1:1 titration with sodium hydroxide gave a dianion with a much broader Soret band ($\Delta\lambda^1/_2 = 75$ nm) at 467 nm. Isosbestic points were again observed (Figure 9a). The *ms*-tetramethylpyridinium porphyrin **4a** showed a similar spectroscopic behavior (Figure 9b). The spectrum does *not* correspond to a monomeric anion (PH^-)[29] but to a polymeric lateral assembly. Both bands at 424 and 452 nm also change in the same manner when after half-titration with sodium hydroxide the aggregation is induced with sodium chloride instead of sodium hydroxide. A similar effect was observed upon diprotonation of anionic TPPS **5a** and was also traced back to lateral aggregation.[30]

Conclusion and Outlook

The porphyrin isomer mixtures **2a**, I−IV or **2a**, III−IV are more soluble in water or water−methanol than the most popular model compound β-octaethylporphyrin is soluble in chloroform. Upon heterodimerization with porphyrin counterions, solubility drops by a factor of 50−100, but 5×10^{-4} M solutions of metalloporphyrin heterodimers can be obtained and are valuable for many purposes. At low concentrations ($\leq 10^{-6}$ M) the large binding constant and at low pH the acid stability of the zinc complex become useful.

The three applications of heterodimers mentioned in the introduction (Figure 1) are currently investigated and depend totally on these properties. Preliminary results are as follows: If vesicles are prepared in a 10^{-6} molar aqueous solution of the isomer mixture **2a**, I−IV from egg lecithin or DPPC by ultrasonication, the fluorescence of **2a** in the bulk medium was totally quenched by a 1.5-fold excess of copper porphyrinate **5b**, whereas the vesicle entrapped porphyrin still fluoresced strongly. Tin(IV) porphyrinate **2d** with a divalent counterion, e.g., sulfate forms fluorescent dimers with zinc porphyrinate **5b** in water. Its photochemistry is currently studied. Molecular monolayers of the free base porphyrin **2a**, II in bulk water (pH 2.5) can be partially capped on the porphyrin edges with copper porphyrin **5b** as detected by partial fluorescence quenching. At lower pH the monolayers dissociate, and fluorescence quenching becomes much stronger. Results of these studies will be reported in due course.

In summary, we have shown here that heterodimers of metalloporphyrins with fitting substituents in *meso*- and β-positions provide pairs of fluorescing and redoxactive dyes with unique properties.

(29) Pasternack, R. F.; Huber, P. R.; Boyd, P.; Engasser, G.; Francesconi, L.; Gibbs, E.; Fasella, P.; Venturo, G. C.; del Hinds, L. *J. Am. Chem. Soc.* **1972**, *94*, 4511.

(30) Tibo, J. M.; Crusats, J.; Rarrera, J.-A.; Valerro, M. L. *J. Chem. Soc., Chem. Commun.* **1994**, 681.

Experimental Section

Spectrophotometric Titrations. Spectroscopic measurements were performed at room temperature with organic solvents of spectrophotometric grade (Fluka) and water of Milli-Q quality in quartz cells (Suprasil) with a Perkin-Elmer Lambda 16 spectrophotometer. Titrations were performed directly in the 1 cm quartz cells in 2 mL volumes by adding small aliquots (4 or 20 μL) of a 10^{-4} M solution to a 2×10^{-6} or 2×10^{-5} M solution. Dilution effects therefore were small enough to allow direct titrations yielding sharp isosbestic points. Titration spectra obtained are not corrected, but the Job-Plots were calculated with actual concentrations using the following formula:

$$F(x) = d(x) - (\epsilon(\beta - \text{porphyrin}) - \epsilon(\text{ms} - \text{porphyrin}))x - \epsilon(\text{ms} - \text{porphyrin})$$

$$d(x) = \frac{A}{c(\beta - \text{porphyrin}) + c(\text{ms} - \text{porphyrin})}$$

$$x = \frac{c(\beta - \text{porphyrin})}{c(\beta - \text{porphyrin}) + c(\text{ms} - \text{porphyrin})}$$

A Perkin Elmer fluorescence spectrophotometer (MPE-44-B) was used for the fluorescence titrations which were performed similarily, but a quartz cell of triangle shape was used to guarantee appropriate transmissions (>80%) at the concentrations of 2×10^{-5} or 2×10^{-6} M. Inner−filter effects could be neglected as was indicated by the correspondance of the absorption and fluorescence excitation spectra. Since the excitation wavelengths were not chosen at isosbestic points, the fluorescence intensity had to be corrected according to the absorption changes to calculate binding constants.

X-ray Structure. Crystals of **1a**,I were obtained from chloroform solutions overlayered with methanol. With respect to the single crystal X-ray structure the most important results are as follows: crystal system: monoclinic; space group *A*2/*a* (no. 15); eight formular units per unit cell; $a = 30.014$ Å (a 90°), $b = 10.731$ Å ($b = 140.53°$), $c = 37.624$ Å ($c = 90°$); final *R* 0.0536. Details are listed in the supporting information.

^{1}H-NMR, IR, and MS data were according to expectation in all cases and are only reproduced here occasionally.

Materials. 2-Nitro-1-pyridin-4-yl-butan-1-ol. 4-Pyridinecarbaldehyde (100 g, 0.934 mol) in 500 mL of toluene was mixed with 300 mL of 1-nitropropane. 1,8-Diazabicyclo[5.4.0]undec-7-ene (DBU) (10 mL) in 50 mL of toluene was slowly added, and the suspension was stirred for 2 days at room temperature and cooled for 2 more days to 4 °C. The crystalline precipitate formed was filtered off, washed with cold toluene, and dried *in vacuo*: yield 165 g (89%); mp 140−145 °C. Anal. Calcd for $C_9H_{12}N_2O_3$ (196.2): C, 55.09; H, 6.16; N, 14.28. Found: C, 55.16; H, 5.93; N, 13.85.

4-(2-Nitrobut-1-enyl)pyridine. The above alcohol (40 g, 0.204 mol) was dissolved in 200 mL of pyridine and slowly mixed with acetic anhydride at 0 °C. The mixture was then stirred at room temperature for 24 hours and at 60 °C for another 6 hours. The solvent was removed. The remaining yellowish oil was dissolved in 80 mL of methanol and crystallized at −18 °C. It was filtered off, washed with cold methanol, and dried at 40 °C: yield 29.7 (81%) of yellowish crystals; mp 62 °C. Anal. Calcd for $C_9H_{10}N_2O_2$ (178.2): C, 60.66; H, 5.66; N, 15.72. Found: C, 60.47; H, 5.44; N, 15.28.

4-Ethyl-3-pyridine-4-yl-2-carbethoxypyrrole. The above but-1-enylpyridine (33.0 g, 0.185 mol) of was dissolved in 370 mL of dry tetrahydrofurane and mixed with 21.0 g (0.186 mol) of isocyanoethylacetate at room temperature. DBU (28.2 g, 0.185 mol) in dry tetrahydrofurane was added dropwise, and the mixture was stirred overnight at room temperature. A brownish precipitate was filtered off, and the solvent was removed from the filtrate. The brownish residue was recrystallized twice from methanol/water: yield 36.5 (81%) of brownish crystals; mp 185 °C. Anal. Calcd for $C_{14}H_{16}N_2O_2$ (244.3): C, 68.83; H, 6.60; N, 11.47. Found: C, 68.77; H, 6.46; N, 11.29.

Sometimes the product did not crystallize because 3-pyridine-4-yl-1*H*-2,4-dicarbethoxypyrrole had been formed as a byproduct. This product must be removed by column chromatography (silica gel, ethyl acetate/hexane = 1:2). The diester is in the second fraction (mp 219 °C).

4-Ethyl-3-pyridine-4-yl-2-hydroxymethylpyrrole. The above pyrrole (10 g) was reduced at 0 °C with 4.32 g (0.113 mol) of $LiAlH_4$ in 500 mL of dry tetrahydrofuran. The mixture was stirred for 2 hours at 0 °C, mixed with 100 mL of ethyl acetate, and poured into 1.15 L of saturated ammonium chloride solution. The product was extracted with ethyl acetate, the organic phases were collected, washed with water, and dried over sodium sulfate, and the solvent was removed. The brownish residue (7.7 g; 93%) was used directly in the following porphyrin synthesis.

Tetraethyl-*β*-tetrapyridine-4-yl-21,23-dihydroporphyrin Isomer Mixture (1a, I−IV) and Isomer Separation. The above pyrrole (7.2 g, 35.6 mmol) in 400 mL of acetic acid was mixed with 9 mL (123.3 mmol) of dimethoxymethane and 1.2 g (7.0 mmol) of *p*-toluenesulfonic acid. The solution became brown and was stirred overnight. 2,3-Dichloro-5,6-dicyano-1,4-benzoquinone (DDQ) (6.1 g, 26.9 mmol) was added, and the dark red solution was stirred for another 5 h. Water (600 mL) was added, and the solution was neutralized with solid sodium bicarbonate and extracted with chloroform. The solvent was removed, and the residue was chromatographed twice over silica gel: first with chloroform/methanol = 9:1 and then with chloroform/methanol = 95:5. The second chromatography gave three separated isomer fractions.

The first fraction contained 590 mg (9.1%) of isomer I: mp > 300 °C; ^{1}H-NMR ($CDCl_3$) δ [ppm] = −3.37 (s, 2H, NH); 1.84 (t, 12H, CH_3); 4.02 (q, 8H, CH_2); 8.07 (d, 8H, 3,5-py); 9.12 (d, 8H, 2,6-py); 10.09 (s, 4H, methine bridges). MS (El, 70 eV, 380 °C) *m*/*z* = 730 (M^+, 100%). Anal. Calcd for $C_{48}H_{42}N_8 \cdot H_2O$ (748.9): C, 76.98; H, 5.92; N, 14.96. Found: C, 76.83; H, 5.79; N, 15.23.

The second fraction (1140 mg, 17.5%) mp > 300 °C contains isomers III+IV. ^{1}H-NMR ($CDCl_3$) δ [ppm] = 9.79, 9.81; 10.07; 10.09; 10.11; 10.44; 10.47 (s, 8H, methine bridges). Anal. Calcd for $C_{48}H_{42}N_8 \cdot H_2O$ (748.9): C, 76.98; H, 5.92; N, 14.96. Found: C, 77.22; H, 5.58; N, 14.75.

The third fraction contained the least soluble isomer II (yield: 130 mg, 2.0%) mp > 300 °C. ^{1}H-NMR (CF_3COOD) δ [ppm] 10.24, 11.32 (s, 2H each, methine bridge). Anal. Calcd for $C_{48}H_{42}N_8 \cdot H_2O$ (748.9): C, 76.98; H, 5.92; N, 14.96. Found: C, 76.68; H, 5.61; N, 14.60.

Zinc Complex (1c) of Isomers, III+IV. The above III+IV isomer mixture (300 mg, 0.41 mmol) was dissolved in 10 mL of hot pyridine and refluxed for 1 h with 100 mg of zinc acetate. The mixture was poured into 200 mL of water and left overnight, and the precipitate filtered off. It was redissolved in chloroform/methanol = 9:1 and chromatographed over silica gel with the same solvent mixture. The eluent was concentrated to a few milliliters and overlayered with methanol. Crystals formed overnight (yield 280 mg; 86%). Anal. Calcd for $C_{48}H_{40}N_8Zn \cdot 1H_2O$ (812.3): C, 70.98; H, 5.21; N, 13.79. Found: C, 70.46; H, 4.98; N, 13.42. After 2 days of drying at 60 °C *in vacuo*: Anal. Calcd for $C_{48}H_{40}N_8Zn$ (794.3): C, 72.59; H, 5.08; N, 14.11. Found: C, 72.89; H, 5.08; N, 13.79.

Copper Complex (1b) of Isomers, III+IV. Same procedure as described for the zinc complex above. Copper(II) chloride (100 mg) was applied for 300 mg of the porphyrin isomer mixture. Anal. Calcd for $C_{48}H_{40}N_8Cu \cdot 1H_2O$ (814.5): C, 71.14; H, 5.22; N, 13.83. Found: C, 71.48; H, 5.00; N, 13.93. After 2 days of drying at 60 °C *in vacuo*: Anal. Calcd for $C_{48}H_{40}N_8Cu$ (792.5): C, 72.75; H, 5.09; N, 14.14. C, 72.58; H, 5.01; N, 13.71.

Tin(IV) Dichloro Complex (1d) of Isomers, III+IV. Tin(II) chloride (3 g) and 3 g of sodium acetate were used for 300 mg of the porphyrin isomer mixture in refluxing acetic acid (300 mL). After reducing the solvent to 100 mL, it was cooled to room temperature, and the precipitate was collected the next day. Chromatography on silica gel with chloroform/methanol/acetic acid = 10:10:1 yielded 345 mg (92%) mp > 300 °C. This compound did not give a satisfactory elemental analysis, but MS still showed Cl^- as axial ligand.

Tetra-(1-methylpyridinium-4-yl)porphyrin Tetrachlorides (2a). The porphyrin (100 mg), e.g., isomer mixture **1a**, III+IV, was dissolved in 25 mL of propan-2-ol by refluxing. Methyl iodide (3 mL) was added. After a few minutes a red precipitate became detectable, and the solution was refluxed for another 3 h. The solution was cooled to −18 °C

overnight and filtered; the residue was dissolved in water and passed four times over Dowex 1×2-400 (chloride). The water was removed, and the residue dissolved in methanol and slowly precipitated again with acetone. The solution was left overnight at room temperature, and the precipitate filtered off and dried *in vacuo* for 2 days at 60 °C. Anal. Calcd for $C_{52}H_{54}N_8Cl_4 \cdot H_2O$ (950.9): C, 65.68; H, 5.94; N, 11.78. Found: C, 65.33; H, 6.54; N, 11.68.

Zinc Complex (2c) III+IV of 2a, III+IV. The nonmethylated zinc porphyrinate isomer mixture (100 mg) **1c**, III+IV was treated as described above for the free base porphyrin. From 100 mg of zinc complex 107 mg of a green amorphous tetramethylation product was obtained (85%). Anal. Calcd for $C_{52}H_{52}N_8Cl_4Zn \cdot 7H_2O$ (1122.3): C, 55.65; H, 5.93; N, 9.98. Found: C, 55.45; H, 5.33; N, 9.68.

Copper(II) Complex (2b), III+IV of 2a, III+IV. Same procedure as above. Yield: 109 mg (87%) of an amorphous, violet powder. Anal. Calcd for $C_{52}H_{52}N_8Cl_4Cu \cdot 8H_2O$ (1138.5): C, 54.86; H, 6.02; N, 9.84. Found: C, 54.71; H, 5.48; N 9.74.

Tin(IV) Dichloro Complex (2d), III+IV of 2a, III+IV. Same procedure as above. Yield: 98 mg (80%) of an amorphous, violet powder. This compound did not give a satisfactory elemental analysis.

Acknowledgment. This work was supported by the Deutsche Forschungsgemeinschaft (SFB 312 "Vectorial Membrane Processes"), the Fonds der Chemischen Industrie, and the Förderungskommission für Forschung der Freien Universität Berlin.

Supporting Information Available: Crystal data and experimental details (4 pages). See any current masthead page for ordering and Internet access instructions.

JA954082G